SPECTROSCOPY FIELD STRATEGIES AND THEIR EFFECT ON MEASUREMENTS OF HETEROGENEOUS AND HOMOGENEOUS EARTH SURFACES

Alasdair Mac Arthur [(1)], Luis Alonso [(2)], Tim Malthus [(3)] Jose Moreno[(4)]
[(1)]NERC FS, Geosciences, Grant Inst., University of Edinburgh EH9 3JW, UK. alasdair.macarthur@ed.ac.uk:
[(2)] Faculty of Physics, University of Valencia, 46100 Burjassot, Valencia, Spain. luis.alonso@uv.es:
[(3)]CSRIO Land and Water, Christian Rd, Acton ACT 2601, Australia. tim.malthus@csiro.au:
[(4)]Faculty of Physics, University of Valencia, 46100 Burjassot, Valencia, Spain. jose.moreno@uv.es:

ABSTRACT

It is assumed in field spectroscopy that the field-of-view (FOV) is defined by a nominal solid angle and that the spectroradiometer's sensitivity to light across the FOV, its Directional Response Function (DRF), displays a 'top hat' or 'Gaussian' response. It has been reported that for two commonly used spectroradiometers these assumptions are erroneous. By generating empirically derived DRF data cubes and convolving these with synthetic Earth surface data cubes the differences between these spectra and those that would have been acquired by the nominal FOV are presented. Furthermore, by simulating different field sampling strategies this paper demonstrates the influence of the DRF on measurements and suggests methods of countering this systematic instrument-induced bias.

1. INTRODUCTION

Field spectroradiometers are portable non-imaging electro-optical devices used to measure spectral reflectance, spectral radiance or spectral irradiance either, generally, through the visible to near infra-red (~0.4μm to ~1μm) or the visible to shortwave infra-red wavelength (~0.4μm to ~2.5 μm) regions of the solar electromagnetic spectrum at ~200 to ~1000 or more sampling intervals. These instruments are used primarily by scientists; a) to gain an understanding of the relationship between spectral features and Earth surface physical state variables and processes; b) for the validation and calibration of data in Earth observation studies or; c) to acquire endmembers for pixel unmixing techniques. To be of scientific value the units of measurement and their absolute physical value must be known to enable measurements to be related to Earth surface state variables and to allow other measurements acquired at spatially and/or temporally distinct periods to be compared. Calibration of measurement devices to national or international norms is the recognised process of standardising such measurements. A number of publications are available which advise on procedures for radiometric calibration and the quantification of electronic system measurement uncertainties. However, little work has been done on characterising the field-of-view (FOV) and spatially related responsivity of field spectroradiometers.

In the spatial sampling of Earth surfaces the 'size, geometry and orientation in space of each area sampled is the support for subsequent analysis [1]. In Earth observation where images are acquired by remote sensing, and where complete coverage of an area is achieved, the support of each measurement is represented by pixels and the measurement recorded is effected by the sensor's point-spread function (PSF) [2, 3]. The PSF of an imaging system is reasonably well approximated by a two-dimensional Gaussian responsivity distribution [4] and this is equally distributed radially. The PSF delimits the area that is sampled and the weighting that the sensor assigns to the radiant flux from each reflecting element within the defined area [3]. It has been demonstrated that the PSF has a significant influence on the information that can be derived from satellite images on a per pixel basis [5]. However, although many sources discuss the characteristics of the PSF and instantaneous field-of-view (IFOV) of imaging systems little research has been published describing the corresponding phenomena for spectroradiometers. The general assumption has been that the FOV of a spectroradiometer, defined by the nominal solid angle specified by manufacturers for each fore optic, delimits the support. Therefore, elements within the support contributing to the measured radiant flux can be identified, quantified and physically sampled. That the area delimited by the FOV is considered to define the support for subsequent analysis is demonstrated when; elements within the instrument's FOV [6, 7]; the diameter of the FOV [8, 9]; the ground FOV[10, 11]; the footprint [12, 13]; and the area observed by the sensor [14, 15] are discussed.

It has previously been demonstrated that the FOVs of two commonly used spectroradiometer/fore optic systems, a GER3700 and an ASD Fieldspec Pro, are not adequately or accurately defined by the manufacturer's specified FOV and that the responsivity is not Gaussian or evenly distributed radially [16]. However, no studies have been carried out to investigate the effect that an instrument's DRF (a systematic measurement bias) has on the measurement of heterogeneous Earth surfaces. By empirically deriving then modelling the DRF of two commonly used field spectroradiometer systems with a range of fore optics and convolving these with synthetic spectral Earth surface data cubes an understanding of the effect each instrument's DRF has on reflectance measurements can be gained.

Proc. 'ESA Living Planet Symposium 2013', Edinburgh, UK
9–13 September 2013 (ESA SP-722, December 2013)

2. METHOD

The DRF data of a GER 3700 #1008 and of an ASD Fieldspec Pro #6449 with a selection of fore optics from [16] were used to generate three-dimensional data cubes of each systems' normalised response, with 1 mm spatial pixels and 2,100 spectral bands (400 nm to 2,500 nm), for each spectrometer/fore optic combination. A number of synthetic Earth surface spectral data cubes were then generated by classifying three RBG digital photographs of three contrasting Earth surfaces; *Festuca*, a 'homogeneous' class; meadow grassland, a 'heterogeneous' continuous cover class; and Corn, a row crop 'heterogeneous' intermittent cover class (Fig. 1). Each pixel was then classified as one of 17 possible endmembers, listed in Fig. 2, measured during a number of previous field campaigns. These endmembers were not being used here to generate 'real' Earth surfaces but synthetic surfaces with realistic spatial and spectral distributions. The spectra were then assigned to the appropriate classified pixel positions to generate synthetic spectral data cubes, approximately 1.5 m x 1.5

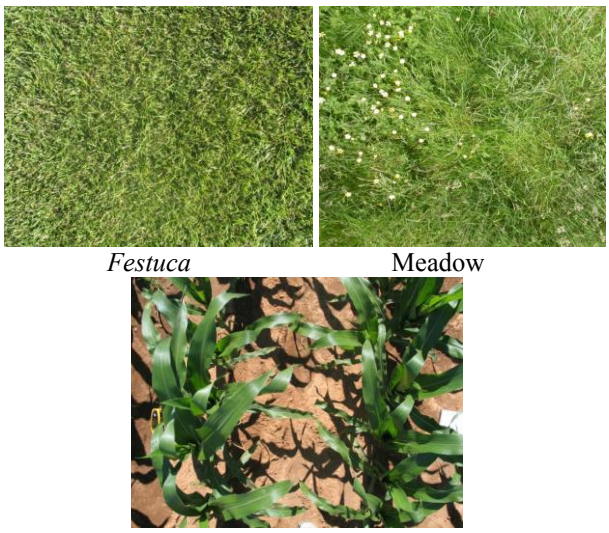

Festuca Meadow

Corn

Figure 1. Examples of Earth surface RGB photos

m with approximately 1 mm pixels and 2,100 spectral bands, for each surface class. Spatial sub sets, with dimensions matching the appropriate DRF cube, of these synthetic Earth surface cubes were then selected by replicating field measurement sampling strategies. The strategies adopted were, random, transect, and smear (i.e. moving the spectrometer fore optic over the Earth surface in a linear direction while the instrument records and averages an integrated measurement). These synthetic Earth surface data cubes were then convolved with each DRF cube and the resulting three–dimensional matrix averaged to generate a simulated spectral measurements. The position of each sub set was selected by generating random numbers and assigning these to 'x', 'y' coordinates on the indexed surface face of the cube. For the random samples these starting points could be anywhere in the indexed surface such that the full cube could be sampled; for the transect random numbers were used to select a starting point on either the 'x' or 'y' axis of the indexed surface and 5 equally spaced samples selected across the image. The smear sample starting point was selected in the same manner as the transect sampling starting point. However, the direction of smear was perpendicular to the corn rows and, to simulate the continuous measurement, the DRF cube was 'stepped' across the image in 1 pixel increments and 5 averages were the computed from this data. 'Top hat' responsivity (where all spatial positions within the FOV are assumed to have equal spectral weighting in the integrated measurement recorded) data cubes were also generated. These 'top hat' data cubes, were then used to sample the synthetic Earth surfaces using the same sampling techniques and the random numbers used with the DRF cubes. The corresponding DRF spectra could then be compared directly to the 'top hat' spectra and the differences between the two considered. In addition, by computing

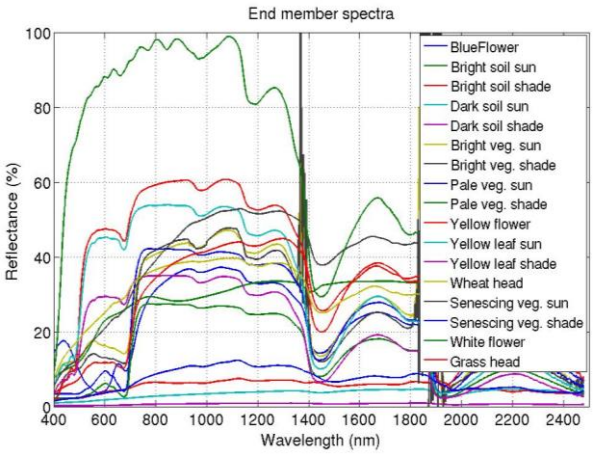

Figure 2. Endmember spectra

the mean spectrum of each image the differences between the image means and the DRF sampled spectra, acquired by each of the different sampling techniques could be compared, indicating how representative the sampled spectra were of larger surface areas. This approach could therefore be used to simulate acquiring spectral endmembers and to assess how representative they were of a larger area.

3. RESULTS AND DISCUSSION

3.1 Spectral variability using different fore optics and measurement strategies

When the random sampling approach was simulated, as was expected, the least variability, indicated by the standard deviation (S.D.) of the simulated measurements, was from the *Festuca* images and the largest from the Corn images. The S.D. for the GER3700 with 10^{o} fore optic DRF spectra simulated from the *Festuca* images was approximately 5% and 4% for the ASD with 10^{o} fore optic, both for n = 9 at 710

nm (the approximate position of the red edge). These S.D. values varied with wavelength and the S.D. values for the other spectrometer/fore optic system combinations was slightly less but comparable as illustrated in Fig. 3. For the simulated measurements of the Meadow image the S.D. was approximately 8% for n = 9 at 710 nm; and for the Corn images the ASD and GER3700 with 10° fore optic spectra S.Ds were approximately 30% for n = 9 at 710 nm, with the other system combinations having an S.D. slightly smaller

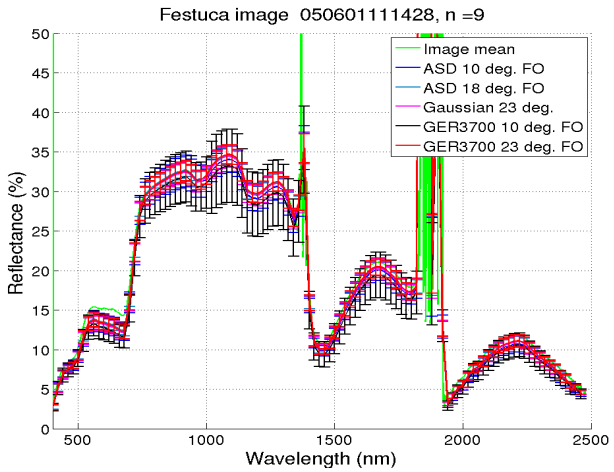

Figure 3. Festuca DRF sample spectra

(Fig. 4). In both these cases the other spectrometer/fore optic system combinations were slightly less but again comparable. The magnitude of the S.D. was wavelength dependent but these reported values were the maximums for *Festuca* and were typical of each image

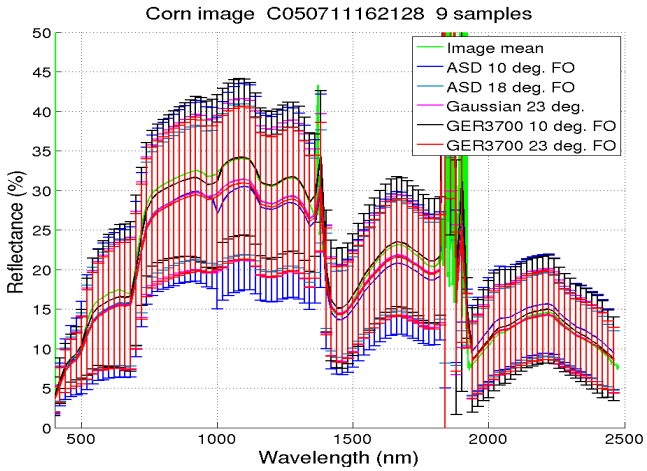

Figure 4 Corn DRF sample spectra

and random sampling starting location. For the *Festuca* simulated measurements when n was increased there was little improvement, the S.D. only reduced to approximately 4.5% at 710 nm, indicating that n = 9 captured the inherent variability of the image. However, when 30 Corn spectral samples were simulated the S.D. reduced to approximately 20%. Therefore, more random samples would be required to compute a representative mean of these Corn images. *Festuca* and Meadow continuous cover classes may therefore be reasonably represented by random sampling with n = 9 but for the non-continuous cover class either many more samples than 30 would be needed or another sampling technique would be required to generate a representative mean from a practical number of measurements. However, when the transect and the smear techniques were used to simulate Corm DRF spectral measurements the S.D. remained of the same order of magnitude as simulated from the Corn random sampling. This indicates that to generate a representative mean, again, more samples would be required or another technique would need to be adopted. It was also noted that spectra from the spectroradiometer/lens-based fore optic combinations continuously had a higher S.D. than those from the ASD with 18° fore optic (FO), GER3700 with bare fibre or the simulated Gaussian response, although from the *Festuca* images the increase in S.D. was of the order of 1% to 2% (Fig. 3 and Fig. 4) . This was as expected from the results presented by [16] where the spectral response across the FOV is not a 'continuous field' and the response has a radial bias for the ASD lens-based F.O. and has a left/right bias and rectangular form for the GER3700 lens-based F.O. For the other fore optics the simulated measurements are integrated over a continuous field, although centre weighted, but with no radial bias.

3.2. Differences between DRF and 'top-hat' simulated spectra by F.O. type

When the simulated 'top hat' spectral measurements are compared with the DRF simulated measurements significant differences between each were evident. When the FOV and DRF simulations centred over the same area of the image surface, representing one measurement sample for each, are considered the differences between the two simulations are again wavelength dependent and of the order of ± 3% for the *Festuca* images; + 0% to 30% for the Meadow images and + 8% to – 30% for the Corn images with the lens based GER F.O. simulated spectral measurement having the greatest difference followed by the ASD lens-based F.O. simulated measurements. These differences and those discussed in the rest of this section are displayed in Fig. 5. However, when 5 simulated measurements of each were generated and averaged the difference between the 'top hat' and the DRF spectra were significantly reduced. The magnitude of the difference was reduced to less than ± 5% but significant wavelength dependencies were still noted. However, when 9 random samples were simulated wavelength dependencies were further reduced and difference of less that 2% were noted except for the Corn images where there was an increase in wavelength dependent differences. When 9 alternative random samples from the Corn image were selected the difference was

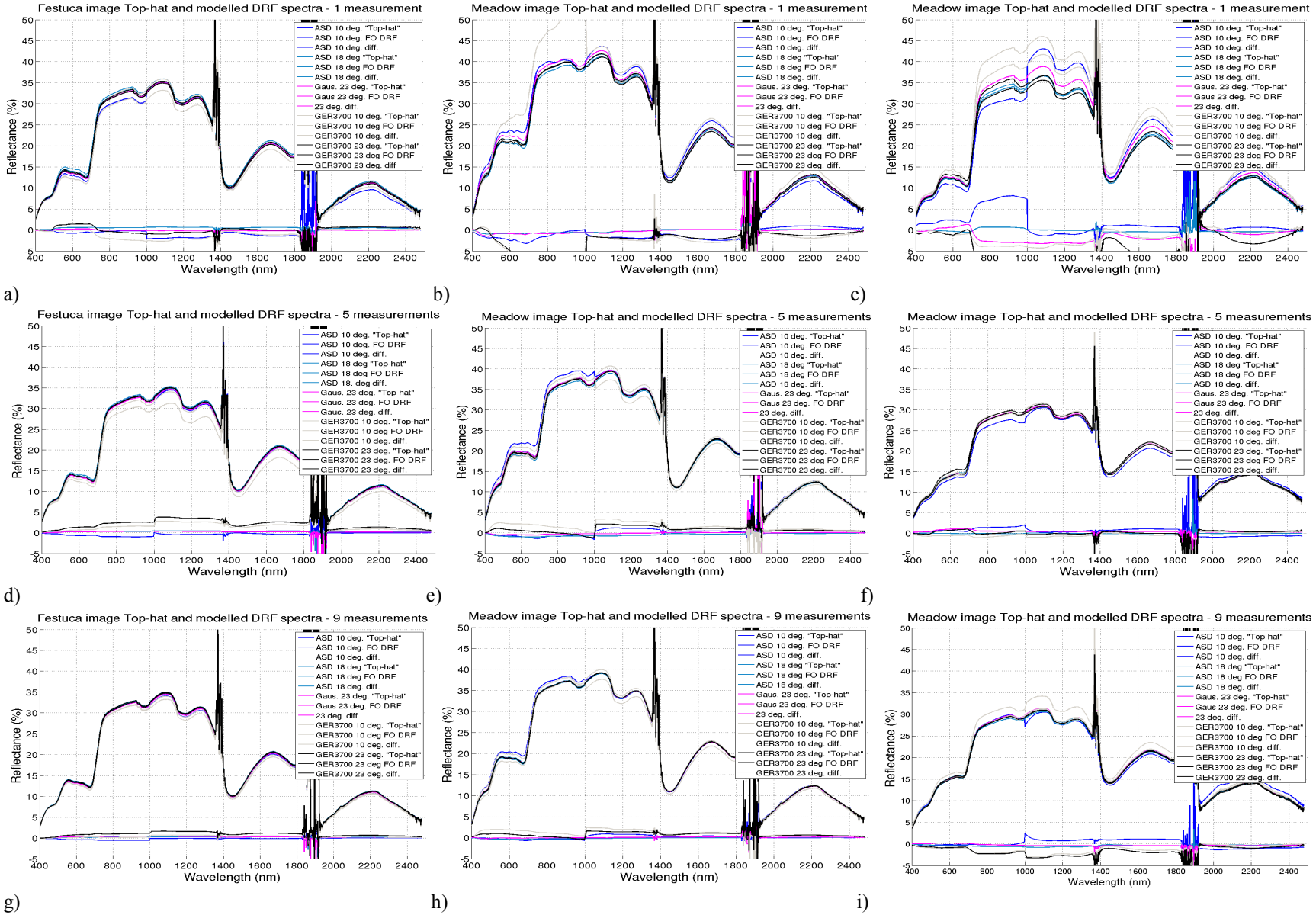

Figure 5. Differences between DRF and 'top-hat' simulated measurements by surface and F.O. type

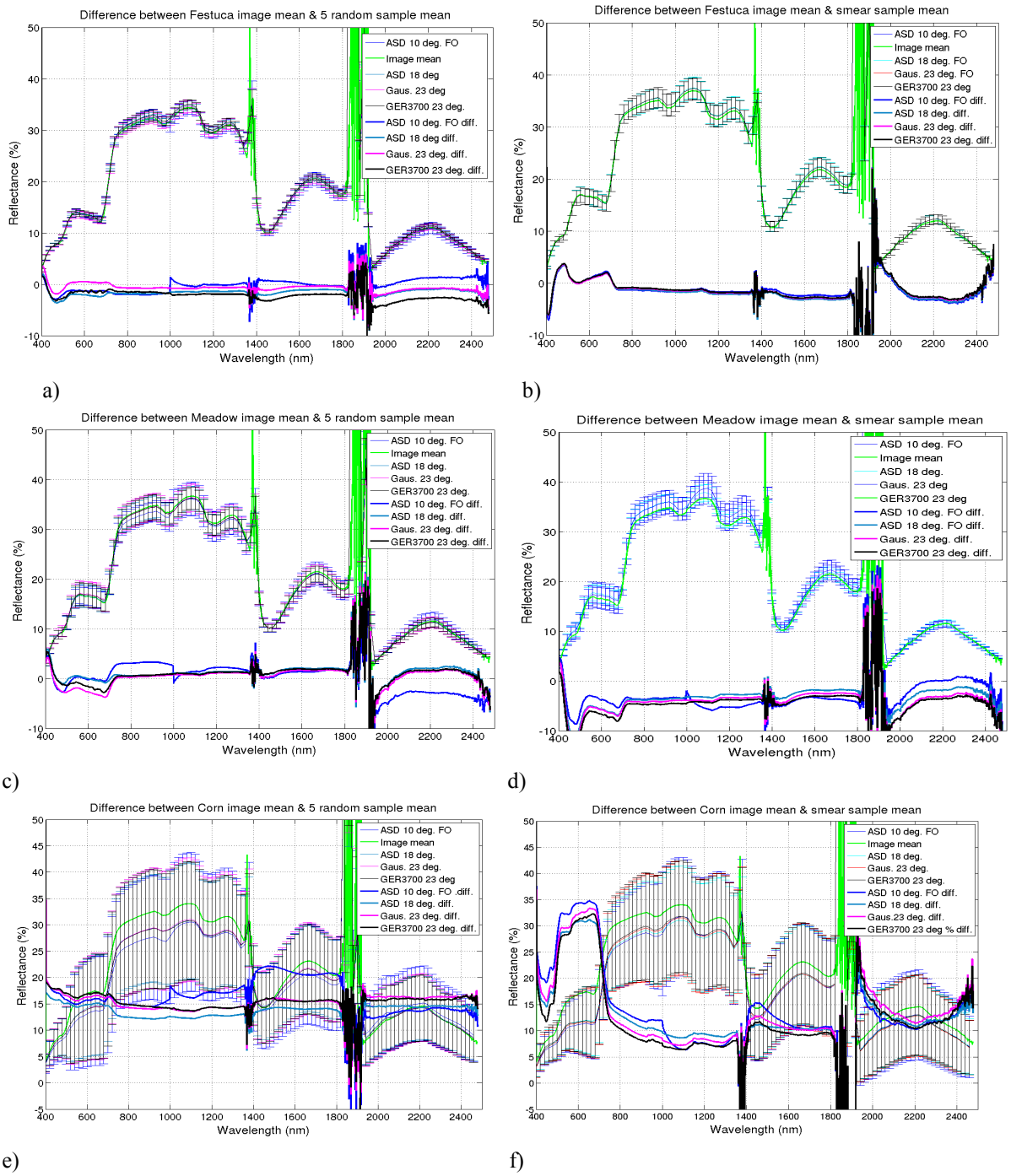

Figure 6. Differences between DRF simulated measurements and mean spectra of one images of each class

comparable to those noted for the other surfaces and when the sampling was increased to 15 and 30 no further improvements were noted. This similarity between the averaged 'top hat' and the DRF spectra is significant. It indicates that if the intention of acquiring field spectroscopic measurements is to establish relationships between spectral features and Earth surface physical properties, physically sampling the surface with the same support as the nominal FOV and making 9 replicates with spectral measurements of the same areas would provide a reasonable spectral mean in which all reflecting elements within the sampled area can considered to have been weighted equally. There were still differences between each of the spectroradiometer/ fore optic combinations but these too were less significant with these sampling techniques.

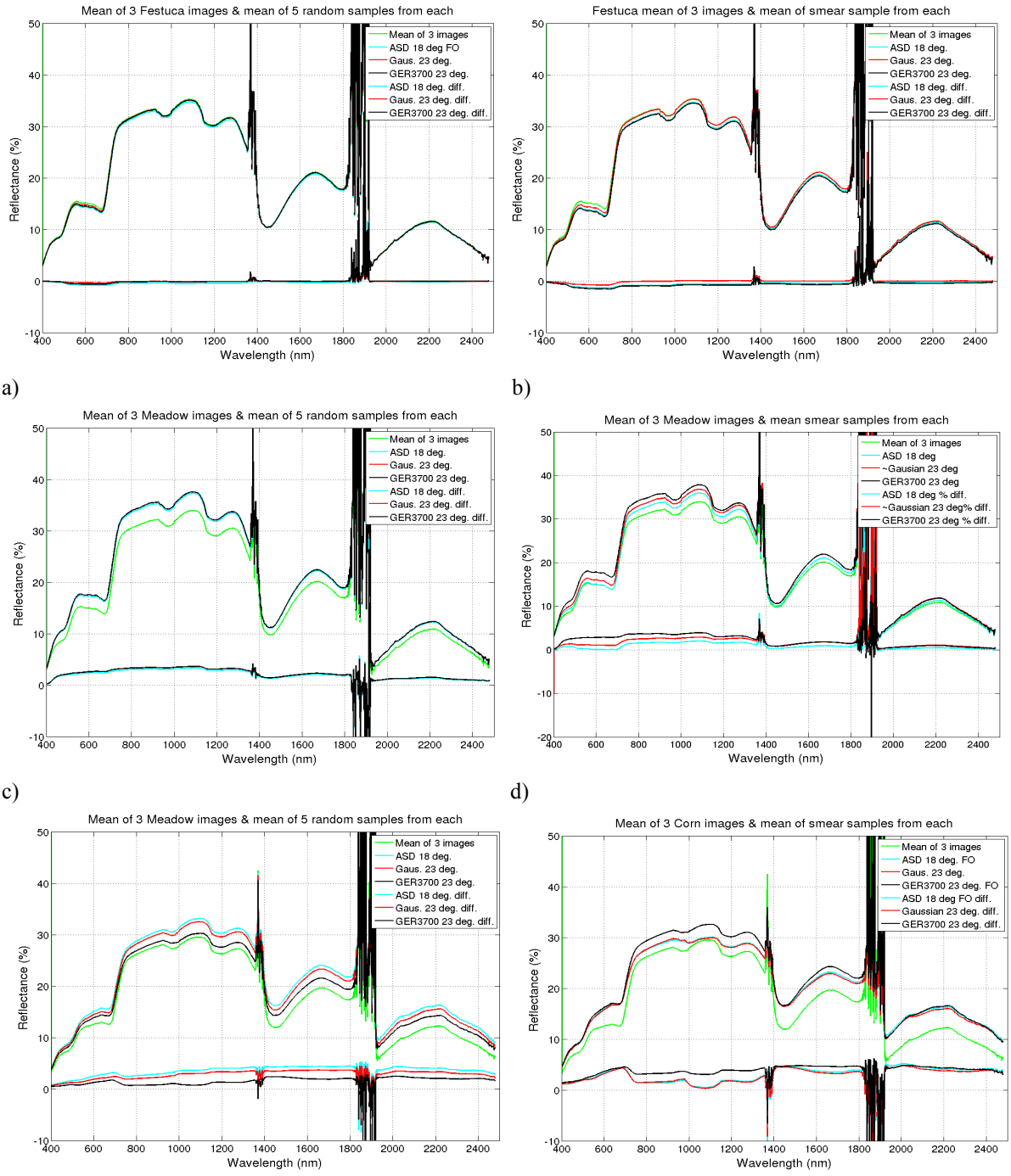

Figure 7. Differences between DRF simulated measurements and mean spectra of 3 images of each class

3.3. Differences between DRF simulated measurements and image mean spectra

The next experiment was to simulate measurements being made to characterise an Earth surface area for Earth observation by optical remote sensing (RS) calibration or validation purposes or to acquire endmembers for RS image analysis. Nine random simulated DRF spectra were averaged, then a 5 sample transect was computed, followed by a 5 averages smear simulation for the fibre-based F.Os. The lens-based fore optics measurements were not simulated due to the variability discussed earlier. The results for the random and smear techniques are presented in Fig 6. The transect simulations showed greater differences than the smear technique so for brevity they have been omitted from further discussion. The differences between both

the random sampling and the smear techniques and the image means for the *Festuca* images are less that ± 5% except at the blue end of the spectra where there was a slight increase to approximately 7% for the smeared spectra, although there were less spectral differences between fore optics. The differences between the Meadow image means and the random sampling simulated DRF spectra were again less than ± 5%, however, the smear simulation had a negative bias across the full spectral range peaking at over 10% between 400 nm and 500 nm. When the simulations for the random sampling and the Corn image means were compared a wavelength dependent difference of between 13% and 23% was observed and this increased to 7 % to 35% for the smear technique, with differences in the visible near infrared region of the spectra being the greatest. This indicates that although random sampling with *n* equal to 9 generates a mean reasonably representative of the image mean for continuous cover surfaces it did not do so for the row crop and the smear technique only did for the most homogeneous surface.

3.4. Differences between DRF simulated measurements and mean spectra of 3 images of each class

In field spectroscopy normally one sample would not be considered adequate to characterise the spectral reflectance of an Earth surface area for RS calibration or validation purposes. Therefore, the means of the three images processed of each surface class were averaged and compared with the averaged means of the simulated DRF measurements generated by the random sampling and by the smear techniques for each surface. For both the random sampling (with *n* equal to 5) and the smear techniques (where *n* also equalled 5) the mean of the simulated measurements of the *Festuca* and the Meadow surface classes were within 3% of the means of each of the surface class images. The maximum difference for the Corn images random sample mean was approximately 3% at 1,600 nm and when the smear technique simulated spectra were compared with the mean of the three Corn images a maximum difference of approximately 5% was noted in the same spectral region.

4. CONCLUSIONS

It appears from this work that without mechanisms to compensate for DRF effects (e.g. the optical mixer to defocus the support imaged onto the fibre bundle, or improved optical components, to minimise aberrations suggested, by [16]) sampling with lens-based fore optics will generally lead to the greatest differences between what the measurement is assumed to represent, the FOV, and the DRF measurement that a spectroradiometer with lens-based FO would make. This is particularly the case for the ASD lens-based system where the S.D. was generally found to be higher, although when only one simulated measurement was made the GER3700 lens-based system displayed the greatest difference. However, for relatively homogeneous Earth surfaces, acceptable results may still be achieved with lens based systems when 5 or more sample are made.

If the aim of a field spectroscopy study is to measure Earth surface reflectance to establish relationships between spectral feature and state variables physically sampled from the surface it may be more advisable to physically sample 9 areas delimited by the spectroradiometer fore optic's nominal FOV and make the spectral measurement of these areas rather than attempt to characterise a larger area (for example the spatial extent of the images used here) and physically sampling that area. However, the validity of this approach relies, as these simulations relied, on random sampling and that requires a robust statistical approach and 'humans' do not do 'random' intuitively.

The transect technique was found to be the least appropriate method for the purposes listed at the start of this work. This technique had neither the statistical validity of the random approach nor the integrated measurement over a larger area of the smear technique.

The differences between the image means and the simulated spectra generated by both the smear technique and by random sampling, with 5 sample simulated to enable a direct comparison between them, displayed great variability when only one image was considered. However, when the mean of the 3 images was computed and compared to the mean of the 5 the samples from each image the maximum difference of approximately 3% was observed for random sampling and approximately 5% for the smear technique. When smearing is used in the field normally lengths greater than 1.5 metres are sampled or more than three areas are sample. Therefore, a more representative mean could be expected, although care has to be taken to smear across rows or an unrepresentative mean may be computed.

It was noted that the step in spectra seen at the region of the detector join at 1,000 nm is due primarily to the DRF as no step was present in the spectra used as endmembers in this work nor was it observed in the 'top hat' spectra. It is therefore primarily being introduced by the spatially dependent spectral weighting of the DRF.

It is also considered that there is a need to increase the area over which measurements are integrated for RS calibration and validation and endmember purposes so that the near-ground measurement support is of the same order of magnitude as the support for satellite sensor measurements. For RS sensor ground sampling distances of up to 30 metres this is now possible using field spectrometers mounted on rotary-wing unmanned

aerial vehicles (UAVs). These offer platforms from which measurements can be made at increased heights and hence make measurements with increased support. In addition, statistically robust random sampling techniques could be implemented as these UAVs can be programmed to fly to pre-determined way points and the co-ordinates of these could be provided by computed program generated random numbers.

This work is an initial investigation and a greater number of Earth surface types, with a more extensive study, including simulate measurements from UAVs, and rigorous statistical analysis would be required prior to firm recommendations being made. For this work a 3% difference was considered reasonable as this is lower than the uncertainty that may be introduced in atmospheric correction processing of hyperspectral images or through general uncertainties (illumination condition variability, for example) and this was used as the threshold criteria. However, for many studies a 5% uncertainty may be what can be achieved in practice.

REFERENCES

1. Atkinson, P. M. and N. J. Tate (2000). "Spatial scale problems and geostatistical solutions: A review." Professional Geographer **52**, 607- 623.

2. Atkinson, P. (2004). Resolution Manipulation and Sub-Pixel Mapping. Remote Sensing Image Analysis: Including the Spatial Domain. S. M. De_Jong and F. D. Van_Der_Meer. London, Kluwer. **5**, 51 - 70.

3. Atkinson, P. M. and P. Aplin (2004). "Spatial variation in land cover and choice of spatial resolution for remote sensing." International Journal of Remote Sensing **25**, 3687-3702

4. Billingsley, F. C., P. A. Anutu, J. L. Carr, C. D. McGillem, D. M. Smith and T. C. Strand (1983). Data Processing and Reprocessing. Manual of Remote Sensing. Falls Church, Virginia, American Society of Photogrammetry. **1**, 719 - 788.

5. Huang, C., J. R. G. Townshend, S. Liang, S. N. V. Kalluri and R. S. DeFries (2002). "Impact of sensor's point spread function on land cover characterization: assessment and deconvolution." Remote Sensing of Environment **80**, 203-212.

6. Murphy, R. J., T. J. Tolhurst, M. Chapman and G. A. J. Uunderwood (2005). "Estimation of surface chlorophyll-a on an emersed mudflat using field spectrometry: accuracy of ratios and derivative-based approaches." International Journal of Remote Sensing **26**, 1835 – 1859.

7. Smith, A. M. S., M. J. Wooster, N. A. Drake, F. M. Dipotso, M. J. Falkowski and A. T. Hudak (2005). "Testing the potential of multi-spectral remote sensing for retrospectively estimating fire severity in African Savannahs." Remote Sensing of Environment, **97**, 92 – 115.

8. Castro-Esau, K. L., G. A. Sánchez-Azofeifa and B. Rivard (2006). "Comparison of spectral indices obtained using multiple spectroradiometers." Remote Sensing of Environment **103**, 276 – 288.

9. Ustin, S. L. and M. L. Whiting (2006). Determination of Crop Residue Cover Using Field Spectroscopy. Soil Carbon and California's Terrestrial Ecosystems. Davis, California, Kearney Foundation of Soil Science, Final Report 2005211, 1/1/2006-12/31/2006, 1 - 13.

10. Mutanga, O., A. K. Skidmore and H. H. T. Prins (2004). "Predicting in situ pasture quality in the Kruger National Park, South Africa, using continuum-removed absorption features." Remote Sensing of Environment **89,** 393-408.

11. Harris, A., R. G. Bryant and A. J. Baird (2006). "Mapping the effects of water stress on Sphagnum: Preliminary observations using airborne remote sensing." Remote Sensing of Environment **100**, 363–378.

12. Ferrier, G., K. A. Hudson-Edwards and R. J. Pope (2009). "Characterisation of the environmental impact of the Rodalquilar mine, Spain by ground-based reflectance spectroscopy." Journal of Geochemical Exploration **100**, 11 – 19.

13. Hilker, T., N. C. Coops, S. B. Coggins , M. A. Wulder , M. Brown, T. A. Black , Z. Nesic and D. Lessard (2009). "Detection of foliage conditions and disturbance from multi-angular high spectral resolution remote sensing." Remote Sensing of Environment **113**, 421 – 434.

14. Darvishzadeh, R., A. Skidmore, M. Schlerf and C. Atzberger (2008). "Inversion of a radiative transfer model for estimating vegetation LAI and chlorophyll in a heterogeneous grassland." Remote Sensing of Environment **112**, 2592 – 2604.

15. Sandmeier, S. R. (2000). "Acquisition of Bidirectional Reflectance Factor Data with Field Goniometers." Remote Sensing of Environment **73**, 257-269.

16. Mac Arthur, A.A., MacLellan, C. and Malthus, T.J. (2012). The fields of view and directional response functions of two field spectroradiometers. Transactions on Geoscience and Remote Sensing, **50**, 3892-3907.